Chemical Physics Letters 780 (2021) 138899

Contents lists available at ScienceDirect

Chemical Physics Letters

journal homepage: www.elsevier.com/locate/cplett

Research paper

Intermolecular proton transfer assisted 1,4-Michael addition for enediyne conversion to enyne-allene

Yun Ding [a,*], Hailong Ma [a], Baojun Li [a,b], Jianfeng Ma [a], Zhehao Hu [a], Yipeng Zhang [a], Xuhaoxi Wen [a], Aiguo Hu [a]

[a] Shanghai Key Laboratory of Advanced Polymeric Materials, School of Materials Science and Engineering, East China University of Science and Technology, Shanghai 200237, China
[b] Skshu Paint Co., Ltd., Putian 351100, China

ARTICLE INFO

Keywords:
Enediyne
Myers-Saito cyclization
Gibbs free energy
Michael addition

ABSTRACT

The conventional Bergman pathway of enediynes to generate diradicals has to overcome a high reaction barrier, which limits the design of enediynes embedded inside a highly strained ring. Here, we proposed an alternative reaction mechanism. By converting the originally inactive enediyne into enyne-allene through possible 1,4-Michael addition, the low barrier Myers-Saito cyclization was triggered. Although direct addition of water or methanol was impossible due to high activation barrier, the 1,4-Michael addition was feasible with the assistance of intermolecular proton transfer at physiological temperature. This mechanism opens a new strategy in the design of structurally simple acyclic enediynes.

1. Introduction

Enediynes possessing a unique core structure of 1,5-diyne-3-ene have drawn intensive attentions since their discovery from natural microorganisms thanks to the high cytotoxicity towards a panel of human cancer cell lines[1–3]. The high antitumor activity stems from the diradicals generated through cycloaromatization reactions of the specific functional core via the well-known Bergman[4–6] or Myers-Saito mechanism[7–9], which enables DNA cleavage in the double-strand structures by abstracting H atoms from the DNA backbones. Despite of their high antitumor anticancer potential, the scarcity of them being directly extracted from natural sources limits their further in-clinic applications. Taking the most recently discovered uncialamycin for example, only $\sim 300\ \mu g$ was isolated from the surface of a British Columbia lichen[10]. Meanwhile, due to the complicated structure feature of these naturally occurring enediynes, tedious reaction route is normally required in the total synthesis, resulting in a relatively low yield[11–14]. To this end, it is essential to design novel enediyne structures featuring simple synthetic procedures and high cytotoxicity at physiological temperature.

Generally, the core structure of enediynes (EDY) is embedded inside a 9- or 10- membered ring in order to reduce the C1-C6 distance [15–18,10]. As pointed out by Nicolaou *et al.*, the C1-C6 distance has to be in the range of 3.2–3.31 Å in order to undergo spontaneous Bergman cyclization at room temperature[11]. Although this critical distance is further expanded to 3.4 Å by Schreiner *et al.*[19], such requirement is disadvantageous to the development of acyclic enediynes. Nonetheless, in 2015, our group reported a kind of acyclic enediynes with a relatively simple structural design, in which maleimide moiety was installed on the double-bond position Scheme 1[20]. The compound with bulky substituents on the triple-bond termini (EDY **1**) was yielded through simple Sonogashira cross coupling reactions, which showed no reactivity at ambient condition. On the contrary, the hydrolyzed product (EDY **2**) after addition of trifluoroacetic acid (TFA) was able to produce radicals at room temperature Scheme 1 as confirmed by electron paramagnetic resonance (EPR) experiments. The large C1-C6 distance in this acyclic structure indicates that the reaction might go beyond the conventional Bergman mechanism.

Recently, we uncovered a new reaction mechanism for a similar enediyne compound with methylene groups adjacent to the triple-bonds, which revealed that the maleimide moiety promoted the intramolecular tautomerization to convert enediynes into enyne-allenes, where the Myers-Saito mechanism was triggered (MARACA mechanism)[21]. However, the MARACA mechanism does not explain the reaction of EDY **2**, as there is no adjacent H atom at the termini to promote the intramolecular 1,3-proton transfer. Inspired by this work, the reaction mechanism of EDY **2** was revisited. We are interested in

* Corresponding author.
E-mail address: yunding@ecust.edu.cn (Y. Ding).

https://doi.org/10.1016/j.cplett.2021.138899
Received 24 May 2021; Received in revised form 14 July 2021; Accepted 16 July 2021
Available online 22 July 2021

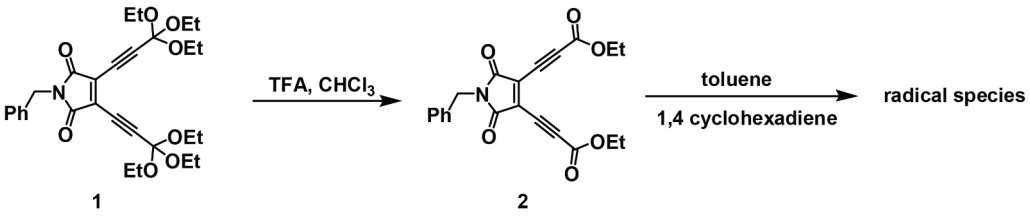

Scheme 1. Reactions of EDY suggested in Ref. [20], where EDY **1** is inactive, while EDY **2** is reactive to generate radical species as confirmed by EPR experiments.

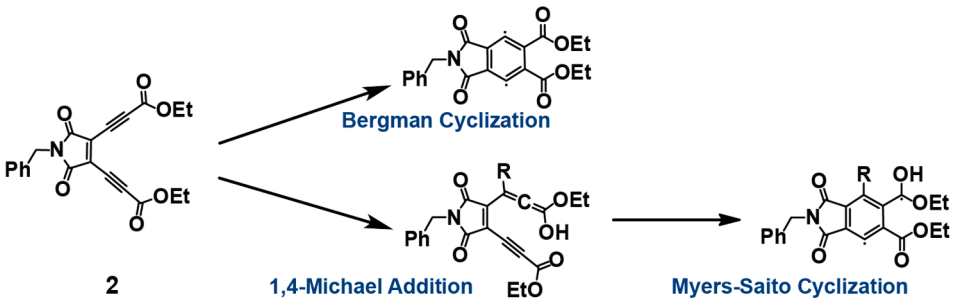

Scheme 2. Possible reaction pathways of EDY **2**.

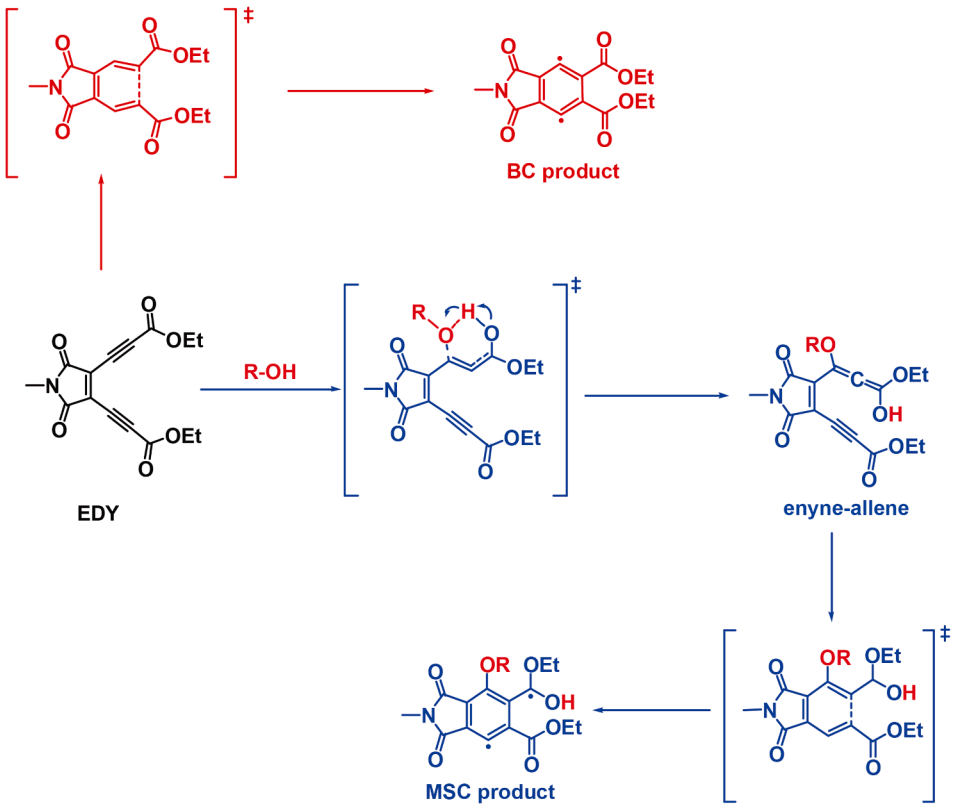

Scheme 3. Possible reaction pathways of model EDY.

how the diradical intermediates were generated without the presence of propargyl group, which would complement the possible reaction pathways in such enediyne structures based on maleimide moiety. Theoretical investigations on the bioactivity of such diradical intermediates could be carried out in the next step.

Considering the unsaturated feature of EDY **2**, which could serve as a Michael acceptor, the possible 1,4-Michael additions to convert enediyne into enyne-allene were proposed and investigated in the presence of either acids or solvent molecules. The Michael addition followed by Myers-Saito cyclization mechanism has already been suggested by Nicolaou *et al.* in the synthesis of Golfomycin A [22]. Our theoretical results indicate that all the direct single molecule additions require high reaction temperature, which is impossible at physiological environment. However, by employing extra molecule working as the catalyst, the solvent molecules demonstrate the ability to achieve successful 1,4-Michael addition at room temperature. The proton shuttle process enhances the $n \rightarrow \pi^*$ orbital interactions, which helps to stabilize the transition state. Meanwhile, the third water molecule anchoring at the

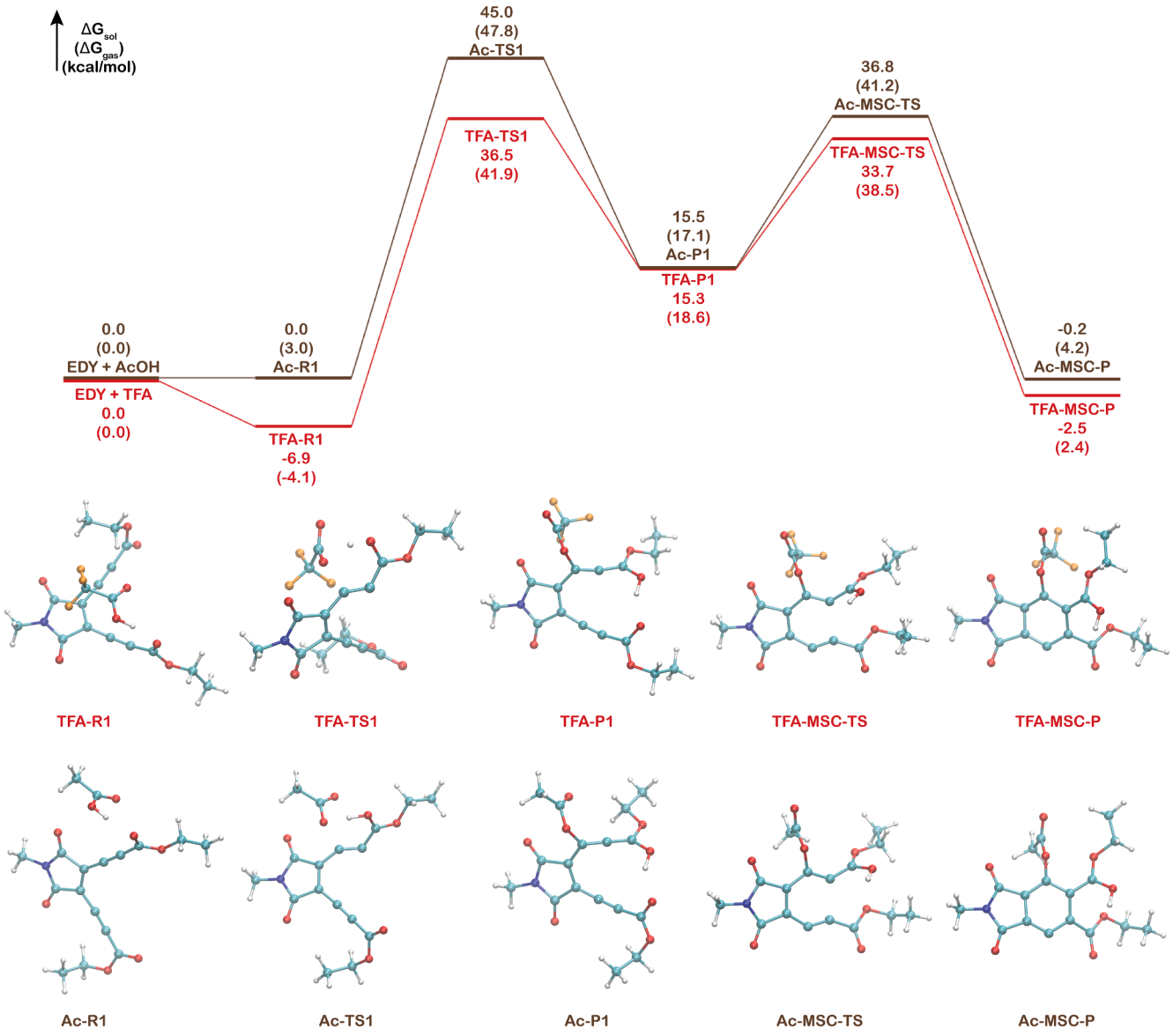

Fig. 1. Energy profiles of TFA or AcOH assisted 1,4-Michael addition, followed by MSC. The Gibbs free energies are reported in both gas phase ((ΔG_{gas})) and the liquid phase (ΔG_{sol}) with PCM description of toluene at 298.15 K. The typical structures are represented in CPK model with C in cyan, N in blue, O in red, F in orange and H in white.

maleimide moiety is proved necessary to achieve successful concerted proton transfers. This work provides deeper insights into the reaction mechanisms of the diradical generation process, which is beneficial for the rational design of new enediyne structures with high antitumor anticancer activity in the near future.

2. Computational methods

The Gaussian 09[23] package was employed to carry out all the calculations. The geometry optimizations were first performed at B3LYP/6-31G* level with Grimme's D3 dispersion correction[24]. Although the open-shell characteristic of the diradical product resulted from Myers-Saito cyclization (MSC) mechanism makes the DFT calculations challenging, the Gibbs activation barriers obtained in this work are all from closed-shell structures. In the previous computational work of Schreiner *et al.*[19,25], pure functional such as BLYP was suggested for the calculations related to enediyne systems, as it was able to produce reaction barriers close to experimental values together with 6-31G* basis set (Please note the obtained reaction free energies from BLYP/6-31G* were still several kcal/mol away from the experimental value [19,25]). However, our tests show that the Gibbs activation energies obtained at B3LYP-D3/6-31G* was close to the ones calculated at BLYP/6-31G* (Table S1). Meanwhile, the computational setup of B3LYP-D3/6-31G* was used in our previous work applied to similar systems, which proved to be accurate enough to provide mechanistic insights into experimental findings[26,21,27,28]. Besides, the B3LYP functional was also employed in other theoretical work related to enediynes[29–34]. Our tests also demonstrated that extra polarization on the hydrogen atoms (6-31G**) only slightly affected the reaction barriers of 1,4-Michael addition, as compared to the barriers obtained from 6-31G* (Table S2).

The Hessian matrices were examined through vibrational frequency analysis at 298.15 K to make sure that the optimized structures correspond to the minima or transition states (TSs) of the potential energy surfaces. Intrinsic reaction coordinate (IRC) calculations were performed at each TSs in gas phase to verify the reaction pathways. The solvent, toluene or methanol was used in the polarizable continuum model (PCM) description[35], where the structures reoptimized from

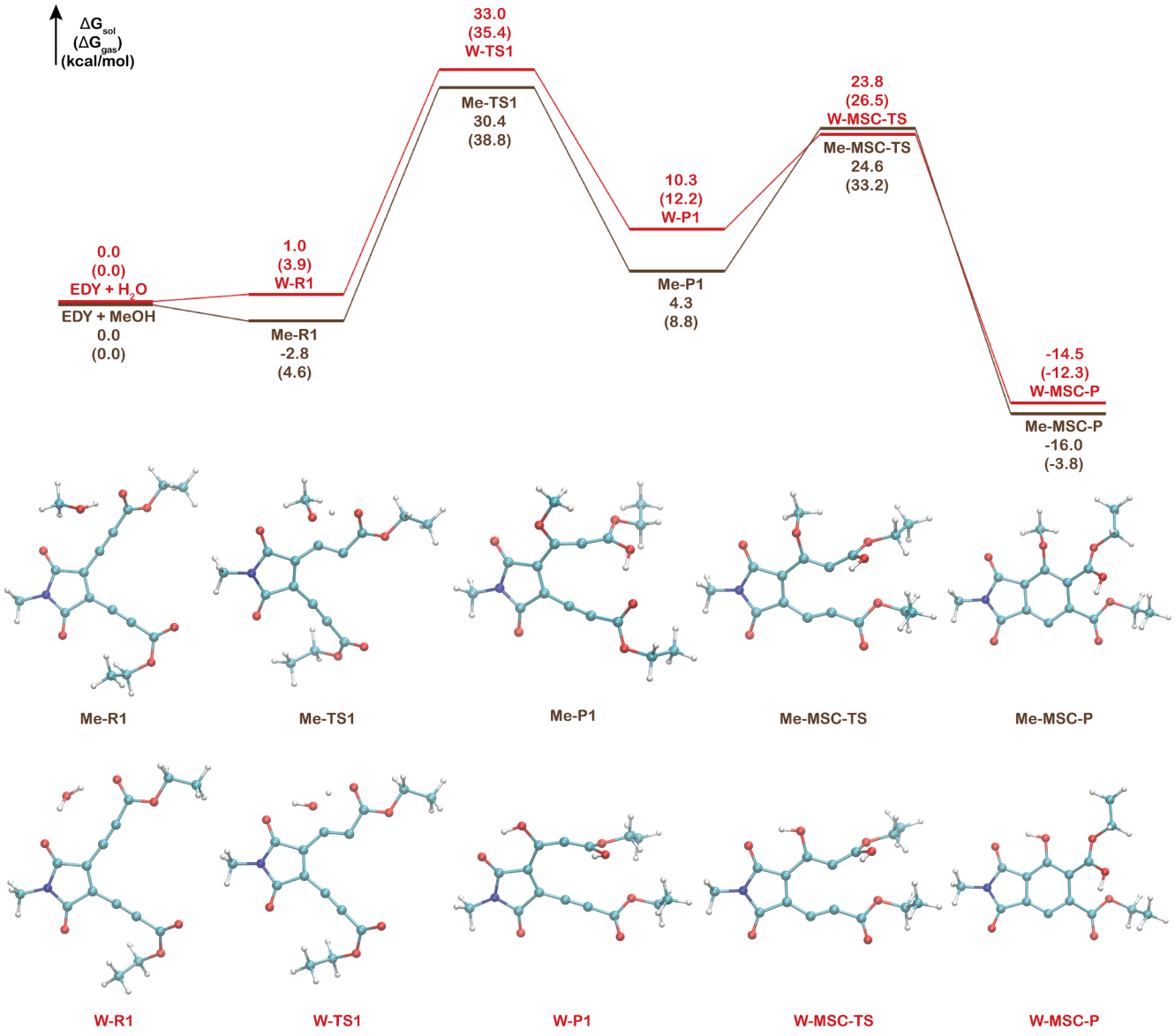

Fig. 2. Energy profiles of water or methanol (MeOH) assisted 1,4-Michael addition, followed by MSC. The Gibbs free energies are reported in both gas phase ((ΔG_{gas})) and the liquid phase (ΔG_{sol}) with PCM description of toluene in water case and methanol in the case of MeOH addition at 298.15 K. The typical structures are represented in CPK model with C in cyan, N in blue, O in red and H in white.

their correspondent gas phase ones. Due to the conversion from closed-shell to open-shell along the BC or MSC pathway, the optimizations of TSs and diradical products, as well as the corresponding IRC calculations were performed with UB3LYP functional with broken symmetry ansatz [36] that is a common approach to treat diradicals generated from enediynes and provides good results[31,33,34]. It is worthy noting that all the TSs display a closed-shell characteristic.

For the 1,4-Michael additions, the numbers of reactants and products are not equivalent. Consequently, the entropic change contributes significantly to the activation free energy barriers, which is the case in gas phase. However, in liquid phase, the translational motions of the solutes are strictly restrained by the surrounding solvent molecules. As a result, the traditional Sackur-Tetrode equation failed to provide the accurate translational entropy. The corrections to the translational entropies[37] were employed in the Gibbs free energies obtained in the solvents; meanwhile, the change of pressure and volume (ΔPV) was omitted. The natural bond orbital (NBO)[38–41] analysis was carried out for structures along the IRC curves in water additions with NBO 3.1 module[42] embedded in Gaussian 09[23], where second order perturbation theory was employed to estimate the orbital–orbital interactions.

Extra single point energy calculations in toluene were carried out at the higher level of (U)B3LYP-D3/6–311+G(2d,p) for the reactions with the lowest barriers. The single point energies were based on the structures optimized at (U) B3LYP-D3/6-31G* in the implicit solvent of toluene. The Gibbs free energies at the higher lever were obtained from the correspondent electronic energies and the thermal corrections at (U) B3LYP-D3/6-31G*.

3. Results and discussion

3.1. Possible reaction mechanisms

The possible reaction pathways of EDY **2** are illustrated in Scheme 2. It involves the direct cycloaromatization following the Bergman cyclization (BC) mechanism or the indirect Myers-Saito cyclization (MSC) through the conversion of EDY to enyne-allene by means of 1,4-Michael addition. To reduce the computational cost, the phenyl substituent at the

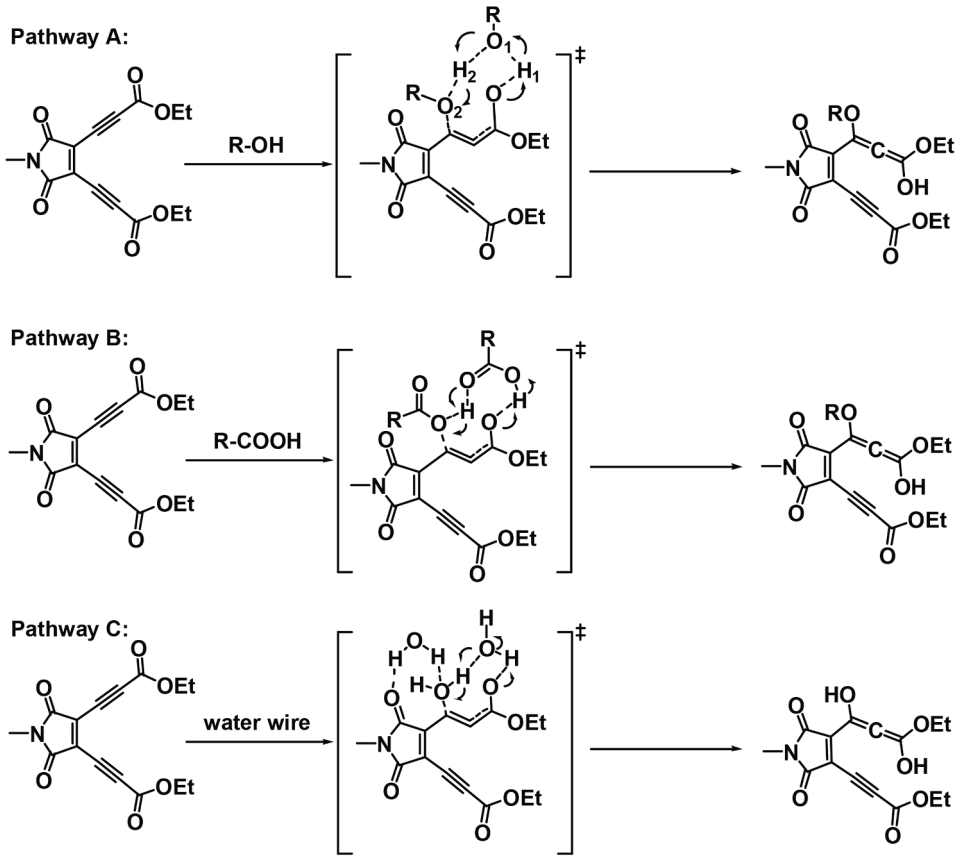

Scheme 4. Possible reaction pathways considered in the presence of hydrogen bonds formed between the nucleophilic reactants.

maleimide moiety was simplified to a hydrogen atom in the following calculations, and the correspondent EDY has a C1-C6 distance of 4.68 Å.

The well-known Bergman cycloaromatization follows the red pathway in Scheme 3, where 1,4-benzenediyl diradicals are generated. However, according to our calculations, the activation free energy is too high (37.4 kcal/mol in toluene, Figure S1) for such reaction to take place at ambient temperature. Thus, the direct intramolecular cycloaromatization is ruled out, while possible pathways to convert EDY into enyne-allene are taken into account. The usual tautomerization is a promising strategy[21], unfortunately, it is forbidden for this specific EDY due to the lack of H atoms at the substituents adjacent to the yne termini. Alternatively, we turn to potential 1,4-Michael addition reactions at the propiolate site, as indicated by the blue pathway in Scheme 3. The nucleophiles attacking EDY were chosen to be TFA, water and methanol (MeOH), which either existed in the reaction mixture of EDY **2** Scheme 1 or in the following characterization experiments[20]. Meanwhile, acetic acid (AcOH) was evaluated as well as it might be present in the biological environments. All the nucleophiles evaluated have the ability to form hydrogen bond network, which proved to be crucial to lower the reaction barrier as we will discuss later.

3.2. Acid assisted 1,4-Michael addition

The 1,4-Michael addition of either acid to EDY is a concerted but asynchronous process, starting with the protonation of the carbonyl group, followed by the addition of trifluoroacetate or acetate group at the yne site. The energy profiles of 1,4-Michael additions as well as the follow-up MSC reactions in the resulting enyne-allenes are shown in Fig. 1. The complexes formed by the reactants are energetically favoured compared to the separated ones in the case of TFA. Consequently, the corrections to the translational entropies calculated in liquid phase did not affect the activation free energies. The free energy barriers for the addition of either acid to EDY are too high to overcome at the physiological temperature, 43.4 and 45.0 kcal/mol for TFA and acetic acid, respectively, which suggests that the function of acid is simply to accelerate the hydrolysis of the bulky groups installed on the non-reactive EDY **1**. Meanwhile, neither fluorine substitutions on the acetic acid nor the non-polar solvent of toluene could significantly alter the activation free energies (46.0 and 44.8 kcal/mol for TFA and acetic acid in gas phase respectively). The huge relative energy differences between the gas phase and the solvent phase mainly stem from the corrections to the translational entropies in toluene.

The activation free energies of MSC reactions are much lower compared to the Michael additions, 18.4 and 21.3 kcal/mol for TFA-P1 and Ac-P1 respectively. So the MSC reaction is feasible once EDY structure is converted to enyne-allene, however the question is that how we can lower the reaction barrier in the first step?.

3.3. Solvent-mediated 1,4-Michael addition

As neither TFA nor acetic acid can react with EDY at room temperature, the simple reactant mixture leaves us the only possibility of solvent at the moment. The 1,4-Michael addition of water or methanol to EDY was concerted but asynchronous as well, however, in contrast to the addition of acids, the nucleophilic addition of anion to the triple bond was prior to the protonation of the carbonyl group. Fig. 2 depicts the energy profiles of water or methanol mediated reactions with regard to EDY. The activation free energies are 35.4 and 33.0 kcal/mol for H_2O addition in gas phase and toluene respectively, while 38.8 and 33.2 kcal/mol for methanol addition in gas phase and methanol respectively. Such activation free energies for 1,4-Michael addition are much lower compared to those of acids (~ 44 kcal/mol), however, considering the relatively low reaction temperature (37 ℃), it is still not feasible. The free energy barriers for MSC is 13.5 and 20.3 kcal/mol after water and

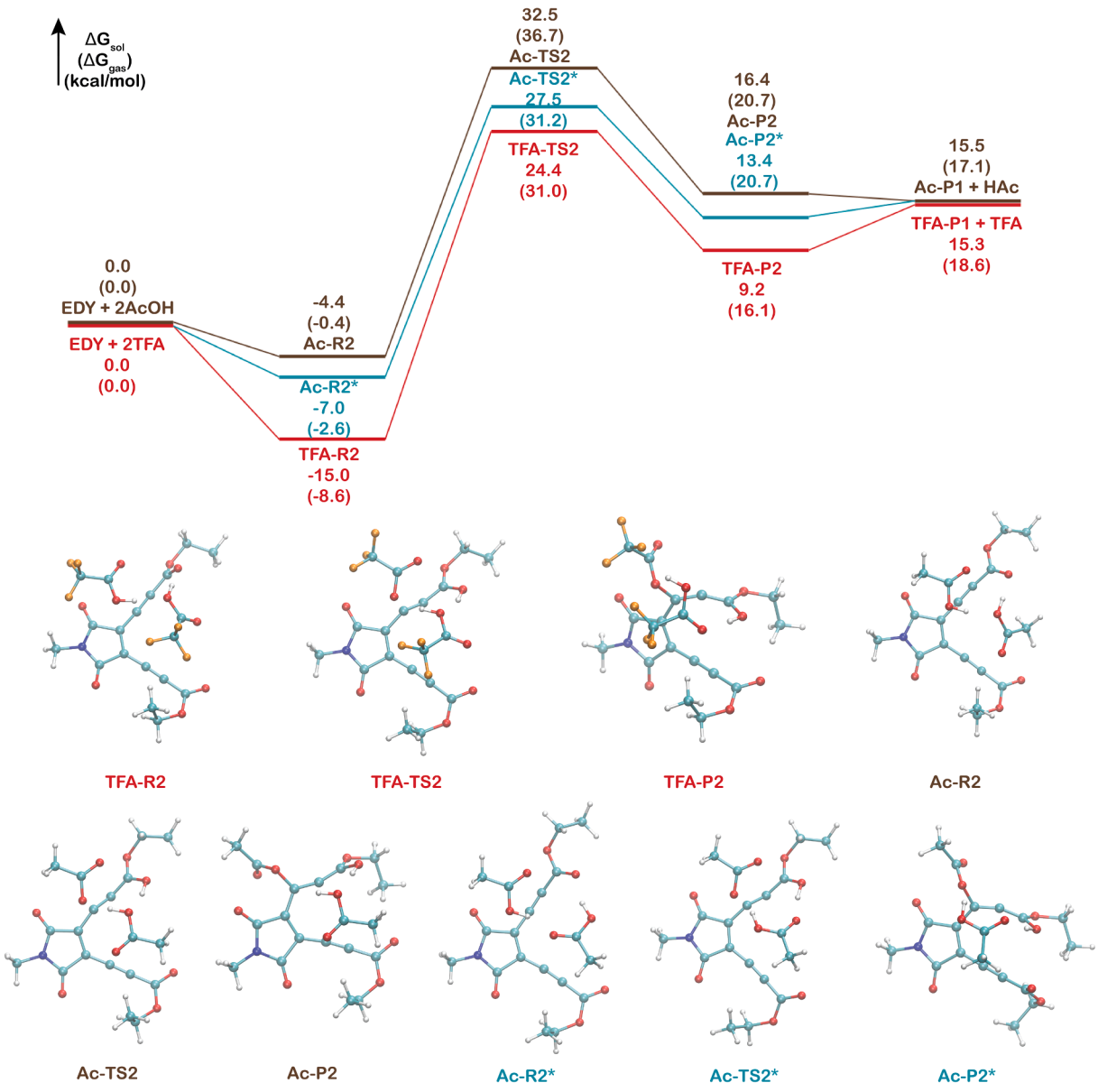

Fig. 3. Energy profiles of 1,4-Michael addition in the presence of two acid molecules. The Gibbs free energies are reported in both gas phase ((ΔG_{gas})) and the liquid phase (ΔG_{sol}) with PCM description of toluene at 298.15 K. The typical structures are represented in CPK model with C in cyan, N in blue, O in red, F in orange and H in white. (For interpretation of the references to colour in this figure legend, the reader is referred to the web version of this article.)

methanol additions respectively. Again, the first step 1,4-Michael addition is the rate-limiting step, and the high reaction barrier hinders the conversion from enediyne to enyne-allene. The successful conversion is essential and the prerequisite to realize the intramolecular cycloaromatization to generate diradical species.

3.4. Proton transfer promoted 1,4-Michael addition

So far, it seems that neither the acids nor the solvents are capable to enable 1,4-Michael addition at the physiological temperature. However, to produce diradical intermediates, it is necessary to transfer enediyne into enyne-allene, so that the lower barrier MSC mechanism is permitted. The common feature of the acids and the solvents examined by now is the ability to form hydrogen bonds among themselves. Inspired by our recent work[28] and the ones in the literature[43,44] that water clusters are able to facilitate the proton or hydrogen atom transfer process, the reaction mechanism of 1,4-Michael addition is investigated in the presence of hydrogen bonds between nucleophiles. The possible pathways are shown in Scheme 2.

In the presence of two TFA or AcOH molecules, the 1,4-Michael addition was assisted through concerted proton transfers (pathway A in Scheme 4), where the protonation of the carbonyl group leads to the proton transfer between two acid molecules, forming one new TFA or AcOH molecule, which could leave the reaction system. The new bonds formation follows the sequence of H_1-O, H_2-O_1, and C-O_2. Such reaction mechanism with extra acid molecule as the catalyst indeed significantly decreases the activation free energies, 39.4 and 36.9 kcal/mol respectively in the addition of TFA and AcOH calculated in toluene Fig. 3. Alternative arrangement of AcOH dimer in Ac-TS2* could further lower the activation free energy (34.5 kcal/mol, pathway B in Scheme 4, Fig. 3), which is attributed to the much stable state of AcOH dimer in this TS configuration (Table S4). In this case, the two proton transfer processes are almost synchronous.

The addition of methanol to EDY is profoundly accelerated with an extra solvent molecule as the catalyst (pathway A in Scheme 4), where the activation free energy decreased by 9 kcal/mol (24.2 vs. 33.2 kcal/

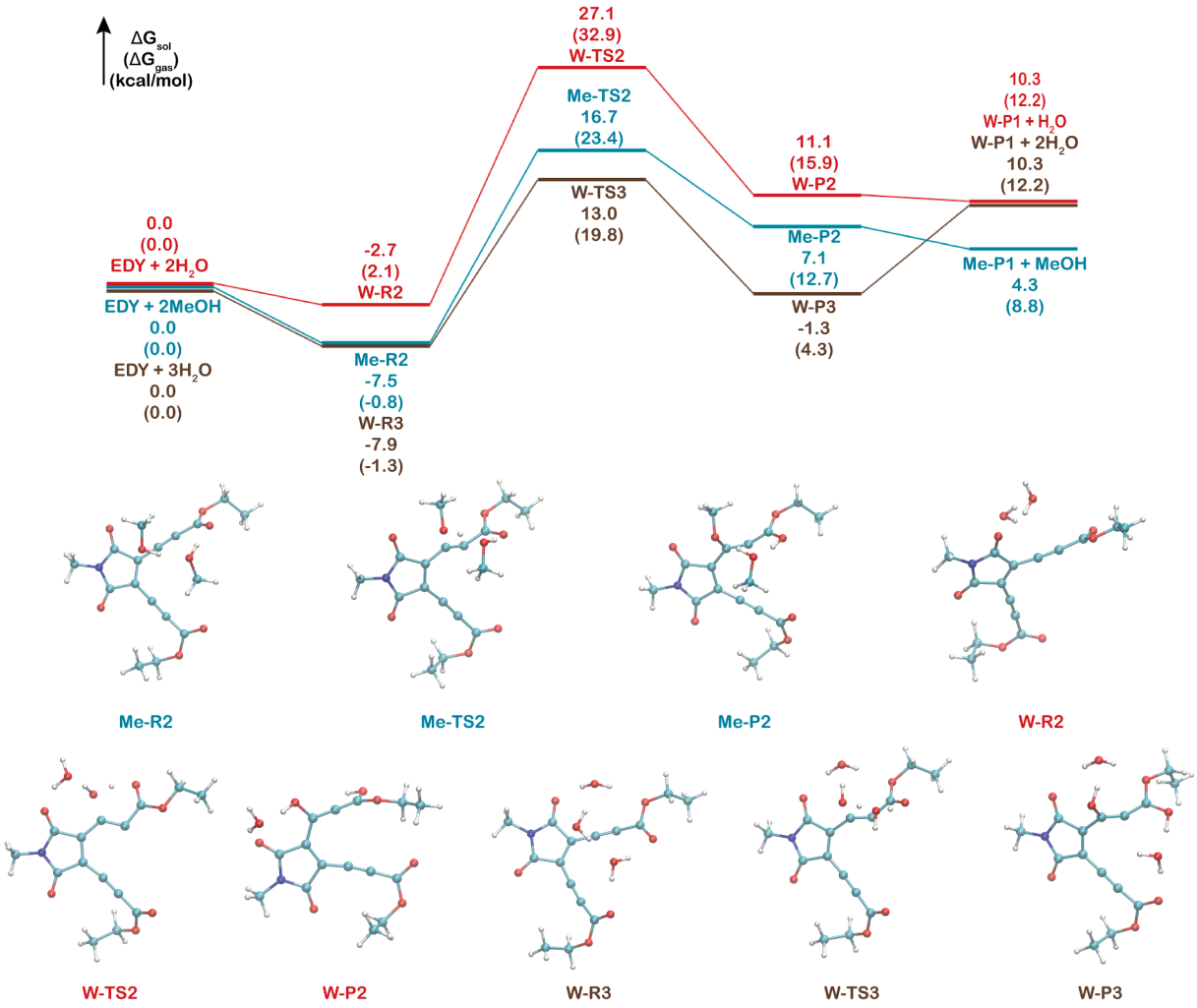

Fig. 4. Energy profiles of 1,4-Michael addition in the presence of solvent molecules. The Gibbs free energies are reported in both gas phase ((ΔG_{gas})) and the liquid phase (ΔG_{sol}) with PCM description of toluene for water addition and methanol solvent for methanol addition at 298.15 K. The typical structures are represented in CPK model with C in cyan, N in blue, O in red and H in white. (For interpretation of the references to colour in this figure legend, the reader is referred to the web version of this article.)

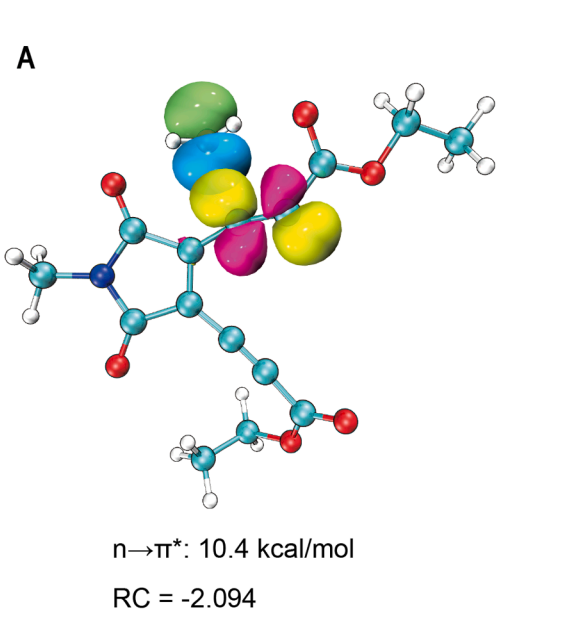

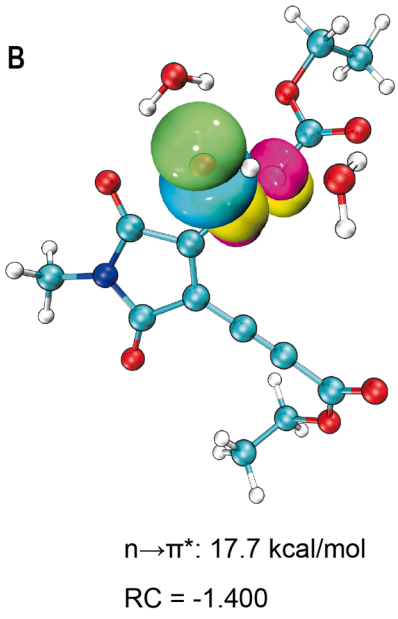

Fig. 5. NBO orbital interactions for structures obtained from the IRC calculations. (A). Structure in single water addition with reaction coordinate (RC) of −2.094. (B). Structure in water wire addition with reaction coordinate (RC) of −1.400. The EDY and water structures are in CPK model, with C in cyan, O in red, N in blue and H in white. The oxygen lone pair orbital is indicated in blue and green lobes, while the π^* orbital is in magenta and yellow lobes. The orbitals are generated at the density of 0.05 a.u. (For interpretation of the references to colour in this figure legend, the reader is referred to the web version of this article.)

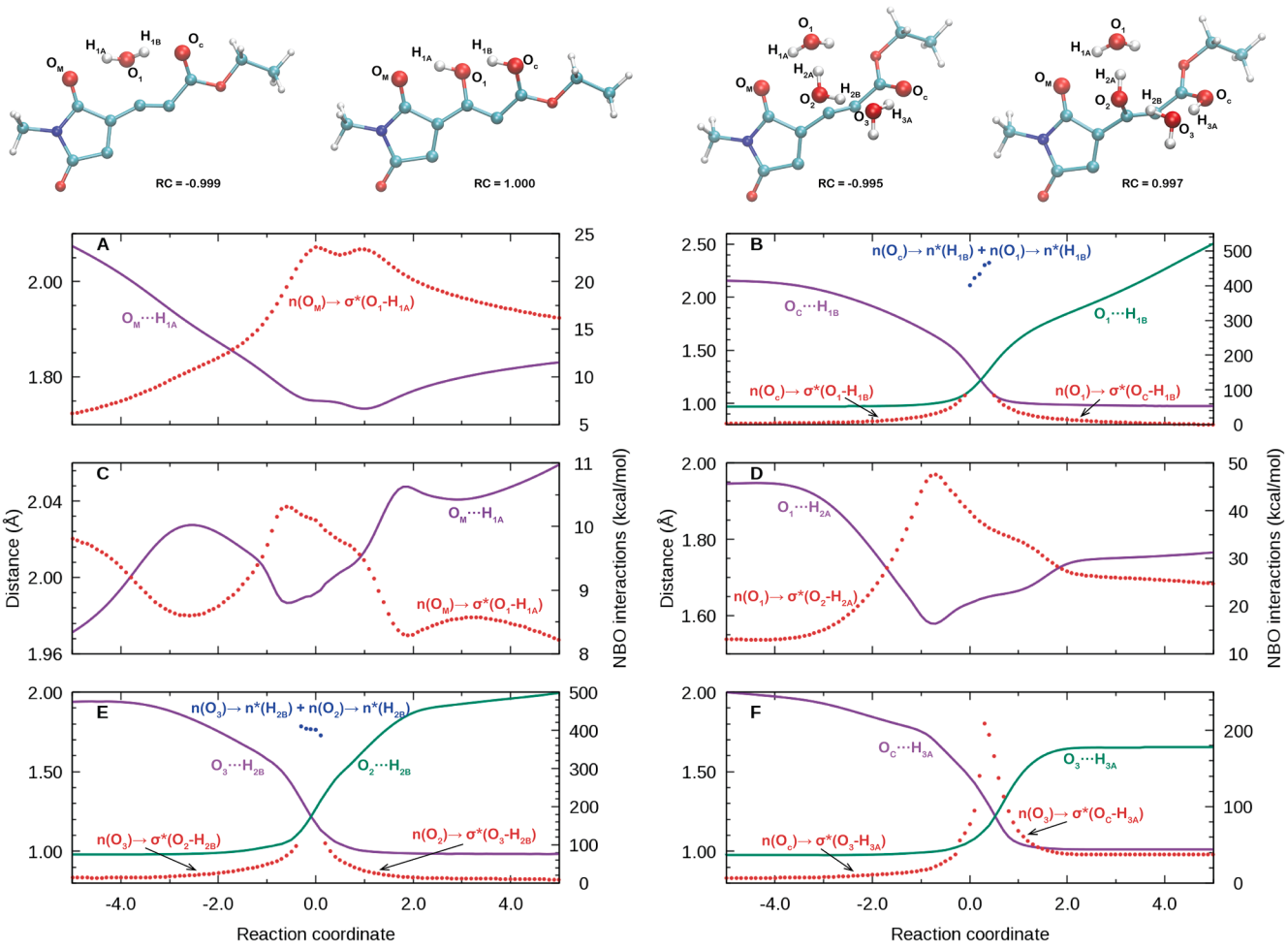

Fig. 6. The distance evolutions of O···H (solid lines) as well as the NBO interactions in the hydrogen bonds along the IRC. (A. B.) Single water addition, where each panel represents one hydrogen bond along the hydrogen bond chain. (C. D. E. F.) Water molecule addition in water wire. The designation of the atoms are illustrated in the CPK representations of the investigated systems with the specific reaction coordinate (RC) values. For clarity, the non-reactive branch substituted on the maleimide moiety is omitted. The purple solid lines represent the distances of the O···H pairs which were originally unbonded, while the green solid lines represent the distances of the originally bonded OH pairs, which undergo proton transfer along the hydrogen bond. The red dots represent the sum of all the n→σ^* NBO interactions in each specific O···H-O hydrogen bond. The blue dots are the n→n* NBO interactions between both O atoms in the hydrogen bond and the proton. (For interpretation of the references to colour in this figure legend, the reader is referred to the web version of this article.)

mol, Fig. 4). However, the new bonds formation follows the reverse sequence of those in the cases of acids, in the order of C-O_2, H_2-O_1, and finally the protonation of the carbonyl group, i.e. the H_1-O bond.

A water cluster of three water molecules was required to achieve concerted proton transfers (pathway C in Scheme 4). In the case of only two water molecules in the 1,4-Michael addition, the extra water failed to work as a proton shuttle, instead, it was anchoring at the carbonyl group in the maleimide moiety as indicated in the structure of W-TS2, forming a hydrogen bond chain, restraining the mobility of the water reactant. Due to the lack of the catalytic effect, the reaction free energy barrier was only slightly reduced, with a value of 29.8 kcal/mol (Fig. 4). The reaction procedure with the water cluster of three molecules is similar to that of methanol, while the extra water molecule anchoring at the maleimide moiety. It is worthy noting that the reduction of the third water molecule in the TS did not lead to a new transition state, which implies that the anchoring water molecule is necessary in such scenario. The resulting free energy barrier of 20.9 kcal/mol is accessible at room temperature, which demonstrates the reaction mechanism of EDY **2** in Ref. [20] as illustrated in the blue pathway of Scheme 3, where 1,4-Michael addition of water to EDY took place first to generate enyne-allene intermediate, which underwent intramolecular Myers-Saito cycloaromatization, producing diradicals. The extremely low MSC reaction barrier of 13.5 kcal/mol and the concerted mechanism in Michael addition prevent the conversion of enol to keto in conventional 1,4-Michael addition process. The energy profiles of the lowest barrier pathways were also evaluated by single point energy calculations at a much larger basis set of 6–311+G(2d,p), and the results are summarized in Table S3. It turned out that the reaction barrier of Michael addition in water wire was quite sensitive to the size of the basis set, with a Gibbs free energy barrier of 27.1 kcal/mol, while the barrier of MSC is 14.9 kcal/mol. Although the barrier of 27.1 kcal/mol is much larger compared to the one calculated at B3LYP/6-31G* with the same solvent condition (20.9 kcal/mol), it is still considered accessible at ambient condition. The effect of larger basis set to the MSC barrier is relatively much smaller (14.9 kcal/mol vs. 12.8 kcal/mol).

3.5. NBO analysis

Intrigued by the huge reaction barrier difference between single water addition and water wire addition, we turn to NBO analysis, in order to have a better understanding at the orbital level. The NBO analysis generates strictly localized orbitals according to Lewis structure description, which resembles the orbital concept in chemistry. Besides, the delocalization of each orbital could be evaluated through second

order perturbation calculations, where the donor–acceptor interaction between bonding and antibonding orbitals tends to stabilize the structure. Interestingly, water molecules interact with different π^* orbitals of C-C triple bond as indicated in Fig. 5: the single water molecule reacts with the π^* orbital parallel to the paper plane, while the water wire consisting three water molecules reacts with the π^* orbital perpendicular to the plane. Such water molecule arrangement in water wire is beneficial for the dihedral angle of O_2-C-C-O (62.2° in W-TS3, see Pathway C in Scheme 2), which is closer to that of the final product W-P1 (91.3°), compared to the value of 24.5° in single water addition (W-TS1). Moreover, the angle of C=C=C is less strained in W-TS3 (126.5° vs. 114.5° in W-TS1), which contributes to the lower reaction barrier as well.

Fig. 6 displays the sum of n→σ^* interactions of each hydrogen bond in single and water wire additions obtained from the structures along the IRC. The O-H distance evolutions are displayed as well. It is striking that the NBO interactions correlate strongly with the unbonded O-H distances. During the proton transfer, the n→σ^* interactions are significantly enhanced in both water addition cases. With the formation of water wire, multiple n→σ^* interaction enhancements further stabilize the separated charge during proton transfer along the longer hydrogen bond chain, which is essential for the much lower reaction barrier. It reveals the importance of water wire in the addition reactions. Such water wire functions as both anchor restraining the water mobility at the reactive site and the charge stabilizer through concerted proton transfers.

4. Conclusion

In conclusion, based on the experimental findings that the maleimide-based acyclic enediyne was able to generate diradicals at room temperature[20], a new reaction mechanism was proposed to convert enediyne into enyne-allene in the absence of adjacent H atoms to the alkyne termini, which was confirmed by DFT calculations. Our work suggests that solvents such as water or methanol could work as Michael donor in the 1,4-Michael addition of enediyne, which only proceeds with the necessary proton transfer between solvent molecules at ambient condition. The low reaction barrier of water addition with the help of intermolecular proton transfer makes the conversion possible in physiological environment, which is essential for the enediyne to generate diradical intermediates through the low barrier MSC pathway. Such mechanism opens a new strategy for the development of acyclic enediynes used as antitumor anticancer antibiotics, which are easier to synthesize compared to the correspondent cyclic ones, but unfortunately generally inactive at physiological temperature due to the high barrier of the conventional Bergman mechanism.

Declaration of Competing Interest

The authors declare that they have no known competing financial interests or personal relationships that could have appeared to influence the work reported in this paper.

Acknowledgement

The authors thank the supports from National Natural Science Foundation of China (21503078) and Natural Science Foundation of Shanghai (20ZR1413400).

Appendix A. Supplementary material

Supplementary data associated with this article can be found, in the online version, at https://doi.org/10.1016/j.cplett.2021.138899.

References

[1] M. Gredicak, I. Jeric, Enediyne compounds - new promises in anticancer therapy, Acta Pharm 57 (2007) 133–150.
[2] R. Romeo, S.V. Giofre, M.A. Chiacchio, Synthesis and Biological Activity of Unnatural Enediynes, Curr Med Chem 24 (2017) 3433–3484.
[3] A.L. Smith, K.C. Nicolaou, The enediyne antibiotics, J Med Chem 39 (1996) 2103–2117.
[4] R.G. Bergman, Reactive 1,4-dehydroaromatics, Acc. Chem. Res. 6 (2002) 25–31.
[5] R.R. Jones, R.G. Bergman, p-Benzyne. Generation as an intermediate in a thermal isomerization reaction and trapping evidence for the 1,4-benzenediyl structure, J. Am. Chem. Soc. 94 (1972) 660–661.
[6] B. Konig, W. Pitsch, M. Klein, R. Vasold, M. Prall, P.R. Schreiner, Carbonyl- and carboxyl-substituted enediynes: synthesis, computations, and thermal reactivity, J Org Chem 66 (2001) 1742–1746.
[7] A.G. Myers, P.S. Dragovich, Design and dynamics of a chemically triggered reaction cascade leading to biradical formation at subambient temperature, J. Am. Chem. Soc. 111 (1989) 9130–9132.
[8] A.G. Myers, E.Y. Kuo, N.S. Finney, Thermal generation of.alpha., 3-dehydrotoluene from (Z)-1,2,4-heptatrien-6-yne, J. Am. Chem. Soc. 111 (1989) 8057–8059.
[9] R. Nagata, H. Yamanaka, E. Okazaki, I. Saito, Biradical formation from acyclic conjugated eneyne-allene system related to neocarzinostatin and esperamicin-calichemicin, Tetrahedron Lett. 30 (1989) 4995–4998.
[10] J. Davies, H. Wang, T. Taylor, K. Warabi, X.H. Huang, R.J. Andersen, Uncialamycin, a new enediyne antibiotic, Org Lett 7 (2005) 5233–5236.
[11] K.C. Nicolaou, Y. Ogawa, G. Zuccarello, E.J. Schweiger, T. Kumazawa, Cyclic conjugated enediynes related to calicheamicins and esperamicins: calculations, synthesis, and properties, J. Am. Chem. Soc. 110 (1988) 4866–4868.
[12] K.C. Nicolaou, H. Zhang, J.S. Chen, J.J. Crawford, L. Pasunoori, Total synthesis and stereochemistry of uncialamycin, Angew Chem Int Ed Engl 46 (2007) 4704–4707.
[13] K.C. Nicolaou, C.R. Hale, C. Nilewski, A total synthesis trilogy: calicheamicin gamma1(I), Taxol(R), and brevetoxin A, Chem Rec 12 (2012) 407–441.
[14] K.C. Nicolaou, et al., Total Synthesis and Biological Evaluation of Tiancimycins A and B, Yangpumicin A, and Related Anthraquinone-Fused Enediyne Antitumor Antibiotics, J Am Chem Soc 142 (2020) 2549–2561.
[15] Y. Ken-ichiro, Y. Minami, R. Azuma, M. Saeki, T. Otani, Structure and cycloaromatization of a novel enediyne, C-1027 chromophore, Tetrahedron Lett. 34 (1993) 2637–2640.
[16] Y. Minami, K. Yoshida, R. Azuma, M. Saeki, T. Otani, Structure of an Aromatization Product of C-1027 Chromophore, Tetrahedron Lett. 34 (1993) 2633–2636.
[17] M. Konishi, H. Ohkuma, T. Tsuno, T. Oki, G.D. VanDuyne, J. Clardy, Crystal and molecular structure of dynemicin A: a novel 1,5-diyn-3-ene antitumor antibiotic, J. Am. Chem. Soc. 112 (1990) 3715–3716.
[18] J.E. Leet, et al., Chemistry and structure elucidation of the kedarcidin chromophore, J. Am. Chem. Soc. 115 (1993) 8432–8443.
[19] P.R. Schreiner, Monocyclic Enediynes: Relationships between Ring Sizes, Alkyne Carbon Distances, Cyclization Barriers, and Hydrogen Abstraction Reactions. Singlet-Triplet Separations of Methyl-Substitutedp-Benzynes, J. Am. Chem. Soc. 120 (1998) 4184–4190.
[20] D. Song, S. Sun, Y. Tian, S. Huang, Y. Ding, Y. Yuan, A. Hu, Maleimide-based acyclic enediyne for efficient DNA-cleavage and tumor cell suppression, J Mater Chem B 3 (2015) 3195–3200.
[21] M. Zhang, et al., Triggering the Antitumor Activity of Acyclic Enediyne through Maleimide-Assisted Rearrangement and Cycloaromatization, The Journal of Organic Chemistry 85 (2020) 9808–9819.
[22] K.C. Nicolaou, G. Skokotas, S. Furuya, H. Suemune, D.C. Nicolaou, Golfomycin A, a Novel Designed Molecule with DNA-Cleaving Properties and Antitumor Activity, Angewandte Chemie International Edition in English 29 (1990) 1064–1067.
[23] Frisch, M.J.; Trucks, G.W.; Schlegel, H.B.; Scuseria, G.E.; Robb, M.A.; Cheeseman, J.R.; Scalmani, G.; Barone, V.; Petersson, G.A.; Nakatsuji, H.; Li, X.; Caricato, M.; Marenich, A.; Bloino, J.; Janesko, B.G.; Gomperts, R.; Mennucci, B.; Hratchian, H. P.; Ortiz, J.V.; Izmaylov, A.F.; Sonnenberg, J.L.; Williams-Young, D.; Ding, F.; Lipparini, F.; Egidi, F.; Goings, J.; Peng, B.; Petrone, A.; Henderson, T.; Ranasinghe, D.; Zakrzewski, V.G.; Gao, J.; Rega, N.; Zheng, G.; Liang, W.; Hada, M.; Ehara, M.; Toyota, K.; Fukuda, R.; Hasegawa, J.; Ishida, M.; Nakajima, T.; Honda, Y.; Kitao, O.; Nakai, H.; Vreven, T.; Throssell, K.; Montgomery, J.A., Jr.; Peralta, J.E.; Ogliaro, F.; Bearpark, M.; Heyd, J.J.; Brothers, E.; Kudin, K.N.; Staroverov, V.N.; Keith, T.; Kobayashi, R.; Normand, J.; Raghavachari, K.; Rendell, A.; Burant, J.C.; Iyengar, S.S.; Tomasi, J.; Cossi, M.; Millam, J.M.; Klene, M.; Adamo, C.; Cammi, R.; Ochterski, J.W.; Martin, R.L.; Morokuma, K.; Farkas, O.; Foresman, J.B.; Fox, D.J. Gaussian 09 Revision E.01. Gaussian Inc: Wallingford, CT, 2016.
[24] S. Grimme, J. Antony, S. Ehrlich, H. Krieg, A Consistent and Accurate Ab Initio Parametrization of Density Functional Dispersion Correction (DFT-D) for the 94 Elements H-Pu, J. Chem. Phys. 132 (2010) 154104.
[25] P.R. Schreiner, A. Navarro-Vázquez, M. Prall, Computational Studies on the Cyclizations of Enediynes, Enyne-Allenes, and Related Polyunsaturated Systems, Acc. Chem. Res. 38 (2005) 29–37.
[26] S. Chen, B. Huang, S. Sun, Y. Ding, A. Hu, Unexpected [2+2] Photocycloaddition between Enediyne Compounds in Solid State, Asian Journal of Organic Chemistry 6 (2017) 775–779.
[27] H. Lu, et al., Facilitating Myers-Saito Cyclization through Acid-triggered Tautomerization for the Development of Maleimide-based Antitumor Agents, Journal of Materials Chemistry B 8 (2020) 1971–1979.
[28] M. Zhang, et al., Experimental and Computational Study on the Intramolecular Hydrogen Atom Transfer Reactions of Maleimide-Based Enediynes After Cycloaromatization, J Org Chem (2020).

[29] A.E. Clark, S. Bhattacharryya, J.M. Zaleski, Density Functional Analysis of Ancillary Ligand Electronic Contributions to Metal-Mediated Enediyne Cyclization, Inorg. Chem. 48 (2009) 3926–3933.
[30] A.G. Lyapunova, et al., Relative Reactivity of Benzothiophene-Fused Enediynes in the Bergman Cyclization, The Journal of Organic Chemistry 83 (2018) 2788–2801. PMID: 29402088.
[31] Q. Nhu, N. Nguyen, D.J. Tantillo, When To Let Go-Diradical Intermediates from Zwitterionic Transition State Structures? J. Org. Chem. 81 (2016) 5295–5302.
[32] A. Basak, S. Das, D. Mallick, E.D. Jemmis, Which One Is Preferred: Myers-Saito Cyclization of Ene-Yne-Allene or Garratt-Braverman Cyclization of Conjugated Bisallenic Sulfone? A Theoretical and Experimental Study, J. Am. Chem. Soc. 131 (2009) 15695–15704.
[33] P.G. Wenthold, A.H. Winter, Nucleophilic Addition to Singlet Diradicals: Homosymmetric Diradicals, The Journal of Organic Chemistry 83 (2018) 12390–12396.
[34] P.G. Wenthold, A.H. Winter, Nucleophilic Addition to Singlet Diradicals: Heterosymmetric Diradicals, The Journal of Organic Chemistry 83 (2018) 12397–12403.
[35] S. Miertu, J. Tomasi, Approximate Evaluations of the Electrostatic Free Energy and Internal Energy Changes in Solution Processes, Chem. Phys. 65 (1982) 239–245.
[36] L. Noodleman, Valence bond description of antiferromagnetic coupling in transition metal dimers, J. Chem. Phys. 74 (1981) 5737–5743.
[37] M. Mammen, E.I. Shakhnovich, J.M. Deutch, G.M. Whitesides, Estimating the Entropic Cost of Self-Assembly of Multiparticle Hydrogen-Bonded Aggregates Based on the Cyanuric Acid·Melamine Lattice, The Journal of Organic Chemistry 63 (1998) 3821–3830.
[38] J.P. Foster, F. Weinhold, Natural Hybrid Orbitals, J. Am. Chem. Soc. 102 (1980) 7211–7218.
[39] A.E. Reed, F. Weinhold, Natural Bond Orbital Analysis of Near-Hartree-Fock Water Dimer, J. Chem. Phys. 78 (1983) 4066–4073.
[40] A.E. Reed, R.B. Weinstock, F. Weinhold, Natural Population Analysis, J. Chem. Phys. 83 (1985) 735–746.
[41] A.E. Reed, L.A. Curtiss, F. Weinhold, Intermolecular Interactions from a Natural Bond Orbital, Donor-Acceptor Viewpoint. Chemical Reviews 88 (1988) 899–926.
[42] Glendening, E.D.; Reed, A.E.; Carpenter, J.E.; Weinhold, F. NBO Version 3.1.
[43] F.-Q. Shi, X. Li, Y. Xia, L. Zhang, Z.-X. Yu, DFT Study of the Mechanisms of In Water Au(I)-Catalyzed Tandem [3,3]-Rearrangement/Nazarov Reaction/[1,2]-Hydrogen Shift of Enynyl Acetates: A Proton-Transport Catalysis Strategy in the Water-Catalyzed [1,2]-Hydrogen Shift, J. Am. Chem. Soc. 129 (2007) 15503–15512.
[44] B. Yuan, R. He, W. Shen, W. Hu, M. Li, DFT Study on the CuBr-catalyzed Synthesis of Highly Substituted Furans: Effects of Solvent DMF, Substrate MeOH, Trace H_2O and the Metallic Valence State of Cu, RSC Advances 6 (2016) 20294–20305.